

# Neural-Network-based Programmable State Feedback Controller for Induction Motor Drive

Lech M. Grzesiak and Bartłomiej Ufnalski

**Abstract**—The paper deals with the design of speed and flux state-space controller for induction motor drive. Linear Quadratic Regulator theory is employed. Optimal controller gain matrix is calculated for a set of operating points. The artificial neural network (ANN) is trained to provide gain matrix for any operating point. Proposed control scheme has been extensively tested in simulation. Results show promising robustness against machine parameters variations. A nonlinear and non-stationary plant control task has been solved with the help of Linear Time-Invariant (LTI) system theory and ANN-based function approximator.

## I. INTRODUCTION

Induction motor drives are the workhorses of modern industry. The induction machine is a nonlinear plant. The most successful control schemes use reference frames aligned with one of the machine fluxes (Field Oriented Control, FOC) or determines the inverter switching states directly from information on flux and torque (Direct Torque Control, DTC) [1], [2]. So called multiscalar models were proposed to achieve independent control of speed and flux without introducing rotating reference frame [3], [4]. Usually, PI regulators are used as a flux, torque and speed/position (or multiscalar variables) controllers. ANN-based on-line trained speed controller was also successfully incorporated to these schemes [5]. There are many guidelines that can be followed during setting the PI's gains. Designers put emphasis on stability, settling time and dumping. For obvious reasons, subject of optimal control is not frequently addressed. The model of electromagnetic part of the motor is non-stationary - it varies with rotor speed. Moreover, the relation between electromechanical part and mechanical part - given by electromagnetic torque - is nonlinear. Thus, optimization of a controller in terms of cost function minimization seems to be interesting. There are some attempts to optimize motor control system with the help of search algorithms like genetic algorithms or particle swarms. Unfortunately, in case of such search algorithms, the system is rather suboptimal than optimal. They provide "good" local minima instead of global one. On the other hand, theory applicable to LTI systems gives analytical solution for regulator gain matrix  $\mathbf{K}$  such as

Lech M. Grzesiak is with the Institute of Control and Industrial Electronics, Warsaw University of Technology, Warsaw, 75 Koszykowa St., Poland, (phone: +48 22 660 51 23; fax: + 48 22 625 66 33; email: lmg@isep.pw.edu.pl).

Bartłomiej Ufnalski is with the Institute of Control and Industrial Electronics, Warsaw University of Technology, Warsaw, 75 Koszykowa St., Poland (phone: +48 22 660 51 20 ext.5; fax: + 48 22 622 69 56; email: ufnalskb@isep.pw.edu.pl).

the state feedback law  $\mathbf{u} = -\mathbf{K}\mathbf{x}$  minimizes the quadratic cost function

$$f_{\text{cost}} = \int_0^{\infty} (\mathbf{x}^T \mathbf{Q} \mathbf{x} + \mathbf{u}^T \mathbf{R} \mathbf{u} + 2\mathbf{x}^T \mathbf{N} \mathbf{u}) dt \quad (1)$$

subject to the system dynamics

$$\dot{\mathbf{x}} = \mathbf{A}\mathbf{x} + \mathbf{B}\mathbf{u}$$

where:  $\mathbf{x}$ ,  $\mathbf{u}$ ,  $\mathbf{A}$ ,  $\mathbf{B}$ ,  $\mathbf{Q}$ ,  $\mathbf{R}$ ,  $\mathbf{N}$  stand for state vector, input vector, state matrix, input matrix, and penalty matrices (for states, controls, and cross-coupling between states and controls) respectively. Resulting controller is known as LQR (Linear-Quadratic state-feedback Regulator). A pole placement technique can be alternatively employed to determine regulator gain matrix. State-space controllers are recognized to give robust control for demanding applications, e.g. [6], [7], [8]. The pole placement (shifting) technique is sometimes used in AC drive systems to adjust dynamics of a selected part of the system, e.g. [9], [10], [11], [12]. Proposed regulator is in some respect similar to the fuzzy state feedback controller (FSFC) reported in [13], [14], [15]. Nevertheless, there are a few major differences between them. Described FSFC assumes that the motor is fed by current-controlled inverter whereas our system incorporates voltage-controlled inverter. In FSFC flux producing current is adjusted outside the state-space controller. Our solution assumes that the whole of the control system is realized as LQR. In FSFC a few (less than ten) local controllers are combined into one global fuzzy state feedback controller. Thus, it should be regarded as suboptimal one. We propose to use thousands of local models evenly covering the operating range of the drive system. State feedback laws for these models are then compressed in one simple feed-forward neural network (FFNN).

## II. CONTROLLER DESIGN

Using space vector description for the cage induction motor, we have:

$$\begin{aligned}
 \underline{u}_s &= R_s \underline{i}_s + \frac{d \psi_s}{dt} + j \omega_{frame} \underline{\psi}_s \\
 0 &= R_r \underline{i}_r + \frac{d \psi_r}{dt} + j (\omega_{frame} - p_b \omega_m) \underline{\psi}_r \\
 \underline{\psi}_s &= L_s \underline{i}_s + L_m \underline{i}_r \\
 \underline{\psi}_r &= L_r \underline{i}_r + L_m \underline{i}_s \\
 J \frac{d \omega_m}{dt} &= T_e - T_{load} \\
 T_e &= \frac{3}{2} p_b (\underline{\psi}_s \times \underline{i}_s)
 \end{aligned}$$

where:  $\underline{u}_s$ ,  $\underline{i}_s$ ,  $\underline{\psi}_s$  - stator voltage, current and flux space vectors,  $\underline{i}_r$ ,  $\underline{\psi}_r$  - rotor current and flux space vectors,  $R_s$ ,  $R_r$ ,  $L_s$ ,  $L_r$  - stator and rotor resistances/inductances,  $L_m$  - mutual inductance,  $\omega_{frame}$  - reference frame angular speed,  $\omega_m$  - rotor angular speed,  $p_b$  - number of pole pairs,  $J$  - moment of inertia,  $T_e$  - electromagnetic torque,  $T_{load}$  - load torque and  $j$  - imaginary unit.

After splitting space vectors (complex variables) into coordinates (real and imaginary parts) in orthogonal reference frame  $OXY$  rotating with  $\underline{\psi}_s$  at speed  $\omega_{frame} = \omega_{\psi_s}$  and with  $\underline{\psi}_s$  aligned with  $OX$  axis, we obtain

$$\begin{aligned}
 \underline{\psi}_s &= \underline{\psi}_{sx} \\
 \underline{\psi}_{sy} &= 0 \\
 \underline{u}_{sx} &= R_s \underline{i}_{sx} + \frac{d \psi_{sx}}{dt} \\
 \underline{u}_{sy} &= R_s \underline{i}_{sy} + \omega_{\psi_s} \underline{\psi}_{sx} \Leftrightarrow i_{sy} = \frac{u_{sy} - \omega_{\psi_s} \psi_{sx}}{R_s} \\
 0 &= R_r i_{rx} + \frac{d \psi_{rx}}{dt} - (\omega_{\psi_s} - p_b \omega_m) \underline{\psi}_{ry} \\
 0 &= R_r i_{ry} + \frac{d \psi_{ry}}{dt} + (\omega_{\psi_s} - p_b \omega_m) \underline{\psi}_{rx} \\
 \underline{\psi}_{sx} &= L_s \underline{i}_{sx} + L_m \underline{i}_{rx} \Leftrightarrow i_{rx} = \frac{\psi_{sx} - L_s i_{sx}}{L_m} \\
 0 &= L_s i_{sy} + L_m i_{ry} \Leftrightarrow i_{ry} = -\frac{L_s i_{sy}}{L_m} \\
 \underline{\psi}_{rx} &= L_r i_{rx} + L_m i_{sx} = \\
 &= L_r \frac{\psi_{sx} - L_s i_{sx}}{L_m} + L_m i_{sx} = \\
 &= \frac{L_r \psi_{sx} + (L_m^2 - L_s L_r) i_{sx}}{L_m} \\
 \underline{\psi}_{ry} &= L_r i_{ry} + L_m i_{sy} = \\
 &= \psi_{ry} = -L_r \frac{L_s i_{sy}}{L_m} + L_m i_{sy} = \\
 &= \frac{(L_m^2 - L_s L_r) i_{sy}}{L_m} \\
 J \frac{d \omega_m}{dt} &= \frac{3}{2} p_b \psi_{sx} i_{sy} - T_{load}
 \end{aligned}$$

Let us introduce, for clarity, the following substitutions:  $a_1 = \omega_{\psi_s}$  (reference frame angular velocity),  $a_2 = \omega_{\psi_s} - p_b \omega_m$  and  $\lambda = L_s L_r - L_m^2$ . This in turn gives:

$$\begin{aligned}
 \underline{u}_{sx} &= R_s \underline{i}_{sx} + \frac{d \psi_{sx}}{dt} \\
 \underline{u}_{sy} &= R_s \underline{i}_{sy} + a_1 \psi_{sx} \\
 0 &= R_r \frac{\psi_{sx} - L_s i_{sx}}{L_m} + \frac{d}{dt} \left( \frac{L_r \psi_{sx} - \lambda i_{sx}}{L_m} \right) + \frac{a_2 \lambda i_{sy}}{L_m} \\
 0 &= -R_r \frac{L_s i_{sy}}{L_m} - \frac{d}{dt} \left( \frac{\lambda i_{sy}}{L_m} \right) + a_2 \frac{L_r \psi_{sx} - \lambda i_{sx}}{L_m} \\
 J \frac{d \omega_m}{dt} &= \frac{3}{2} p_b \psi_{sx} \frac{u_{sy} - a_1 \psi_{sx}}{R_s} - T_{load}
 \end{aligned} \tag{2}$$

Assuming that the reference frame angular velocity  $a_1$  and slip speed  $a_2$  can be estimated from measured signals, and that control system imposes  $\psi_{sx} \approx \psi_s^{ref}$  (for "first"  $\psi_{sx}$  in (2)), we can regard the system as a "linear" one:

$$\begin{aligned}
 \frac{d \psi_{sx}}{dt} &= u_{sx} - R_s i_{sx} \\
 \frac{d i_{sx}}{dt} &= R_r \frac{\psi_{sx} - L_s i_{sx}}{\lambda} + \frac{L_r (u_{sx} - R_s i_{sx})}{\lambda} + a_2 i_{sy} \\
 \frac{d i_{sy}}{dt} &= -R_r \frac{L_s i_{sy}}{\lambda} + a_2 \frac{L_r \psi_{sx} - \lambda i_{sx}}{\lambda} \\
 J \frac{d \omega_m}{dt} &= \frac{3}{2} p_b \psi_s^{ref} \cdot \frac{u_{sy} - a_1 \psi_{sx}}{R_s} - T_{load}
 \end{aligned}$$

This statement is crucial for further design steps. Under these assumptions, we can calculate optimal gain matrices for a set of pairs  $(a_1, a_2)$  and switch softly between them when the operating point changes. It is necessary to add two new state variables  $p_1$  and  $p_2$  to get zero steady state error (achieved by introducing an integral action in the control loop):

$$\begin{aligned}
 \frac{d i_{sx}}{dt} &= -\frac{R_r L_s + R_s L_r}{\lambda} i_{sx} + a_2 i_{sy} + \frac{R_r}{\lambda} \psi_{sx} + \frac{L_r}{\lambda} u_{sx} \\
 \frac{d i_{sy}}{dt} &= -a_2 i_{sx} - \frac{R_r L_s}{\lambda} i_{sy} + \frac{a_2 L_r}{\lambda} \psi_{sx} \\
 \frac{d \psi_{sx}}{dt} &= -R_s i_{sx} + u_{sx} \\
 \frac{d \omega_m}{dt} &= -a_1 \frac{3 p_b \psi_s^{ref}}{2 J R_s} \psi_{sx} + \frac{3 p_b \psi_s^{ref}}{2 J R_s} u_{sy} - \frac{T_{load}}{J} \\
 \frac{d p_1}{dt} &= \psi_{sx} - \psi_s^{ref} \Leftrightarrow p_1 = \int (\psi_{sx} - \psi_s^{ref}) dt \\
 \frac{d p_2}{dt} &= \omega_m - \omega_m^{ref} \Leftrightarrow p_2 = \int (\omega_m - \omega_m^{ref}) dt
 \end{aligned}$$

In order to design state-space controller, we put  $T_{load} = 0$ ,  $\psi_s^{ref} = 0$ ,  $\omega_m^{ref} = 0$ . We have six state variables

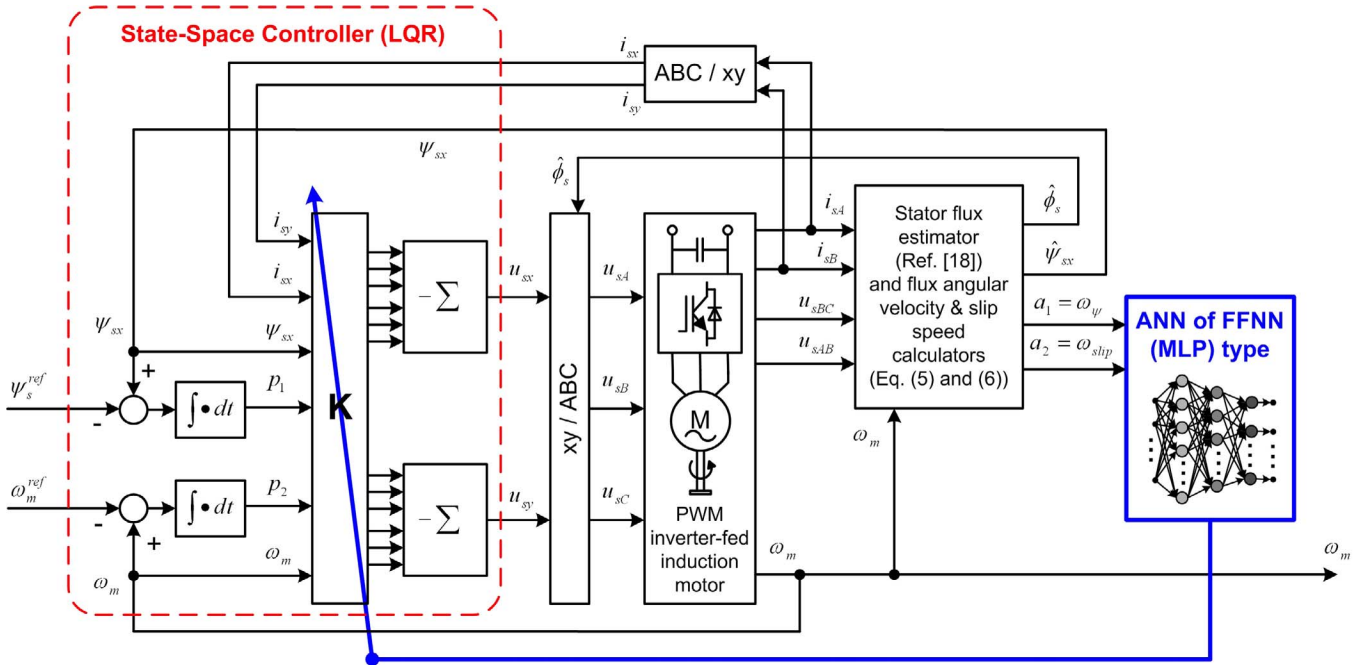


Fig. 1. Schematic diagram of the AC drive with ANN-based programmable state-space controller

$[i_{sx}, i_{sy}, \psi_{sx}, \omega_m, p_1, p_2]$  and two inputs  $[u_{sx}, u_{sy}]$ :

$$\begin{aligned} \frac{di_{sx}}{dt} &= -\frac{R_r L_s + R_s L_r}{\lambda} i_{sx} + a_2 i_{sy} + \frac{R_r}{\lambda} \psi_{sx} + \frac{L_r}{\lambda} u_{sx} \\ \frac{di_{sy}}{dt} &= -a_2 i_{sx} - \frac{R_r L_s}{\lambda} i_{sy} + \frac{a_2 L_r}{\lambda} \psi_{sx} \\ \frac{d\psi_{sx}}{dt} &= -R_s i_{sx} + u_{sx} \\ \frac{d\omega_m}{dt} &= -a_1 \frac{3p_b \psi_s^{ref}}{2JR_s} \psi_{sx} + \frac{3p_b \psi_s^{ref}}{2JR_s} u_{sy} \\ \frac{dp_1}{dt} &= \psi_{sx} \\ \frac{dp_2}{dt} &= \omega_m \end{aligned}$$

This in turn implies the following matrices for LQR method [16]:

$$A = \begin{bmatrix} -\frac{R_r L_s + R_s L_r}{\lambda} & a_2 & \frac{R_r}{\lambda} & 0 & 0 & 0 \\ -a_2 & -\frac{R_r L_s}{\lambda} & \frac{a_2 L_r}{\lambda} & 0 & 0 & 0 \\ -R_s & 0 & 0 & 0 & 0 & 0 \\ 0 & 0 & -a_1 \frac{3p_b \psi_s^{ref}}{2JR_s} & 0 & 0 & 0 \\ 0 & 0 & 1 & 0 & 0 & 0 \\ 0 & 0 & 0 & 1 & 0 & 0 \end{bmatrix}$$

$$B = \begin{bmatrix} \frac{L_r}{\lambda} & 0 \\ 0 & 0 \\ 1 & 0 \\ 0 & \frac{3p_b \psi_s^{ref}}{2JR_s} \\ 0 & 0 \\ 0 & 0 \end{bmatrix}$$

$$Q = \text{diag} \left( \left[ \frac{0.1}{I_N^2}, \frac{0.1}{I_N^2}, \frac{0.002}{\psi_N^2}, \frac{0.1}{\omega_N^2}, \frac{5 \cdot 10^4}{\psi_N^2}, \frac{10}{\omega_N^2} \right] \right) \quad (3)$$

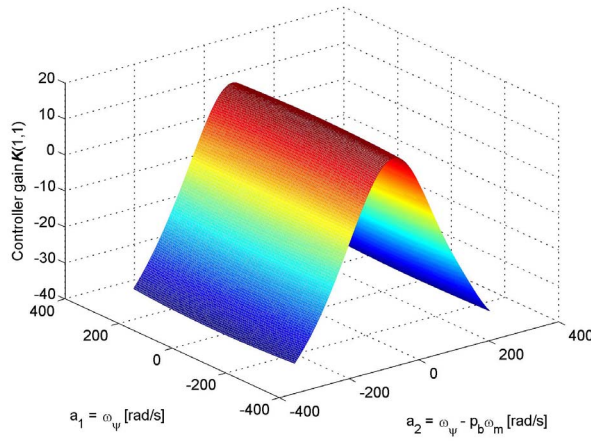
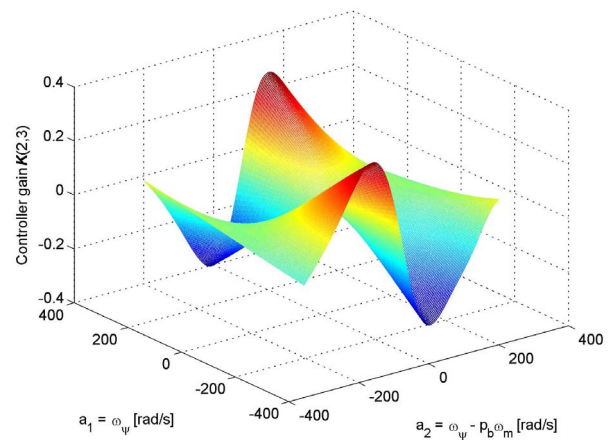
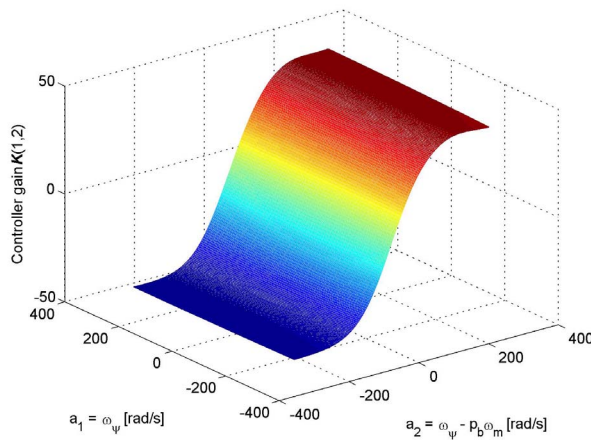
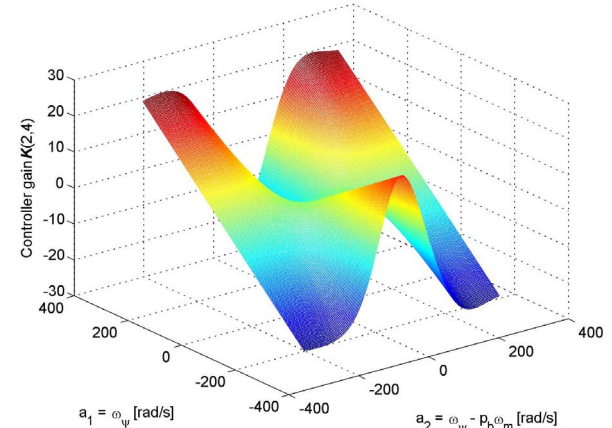
$$R = \text{diag} \left( \left[ \frac{0.01}{U_N^2}, \frac{0.01}{U_N^2} \right] \right) \quad (4)$$

where:  $I_N$ ,  $U_N$ ,  $\omega_N$ ,  $\psi_N$  - nominal values for current, voltage, mechanical speed and flux respectively.

It is common to set  $N$  in (1) equal to zero in most practical control tasks. Penalty coefficients were normalized by dividing the value for each input and state variable by the square of its nominal value. The big value of  $Q$  (5,5) linearizes (2) by imposing  $\psi_{sx} \simeq \psi_s^{ref}$ . Coefficients present in (3) and (4) were applied to induction motor with parameters specified in Table I (see Appendix). It is possible to achieve different dynamic behavior of the drive by playing with those coefficients. After setting  $Q$  and  $R$  (suitably to the requirements of the drive), optimal gain matrix  $K$  is generated for each  $(a_1, a_2) \equiv (\omega_{\psi_s}, \omega_{\psi_s} - p_b \omega_m)$ . Multidimensional modeling of  $K_{[2 \times 6]} = f(a_1, a_2)$  is performed by off-line trained ANN. A multilayer perceptron (feed-forward neural network) with eleven hidden sigmoidal neurons is used. Resulted architecture of the control system is shown in Fig. 1.

### III. SIMULATION RESULTS

Described system was extensively tested in simulation. A detailed model was built in MATLAB/Simulink environment. A power part of the model (i.e. voltage-source inverter fed induction motor) was modelled with the help of software package PLECS [17]. Some key parasitic effects have been simulated, i.e. system and measurement noise, phase lag and amplitude attenuation introduced by hardware filters, small dc-offset at outputs of measurement transducers. Flux estimator was introduced to the model to make practical realization possible. Estimator with amplitude limiter in polar

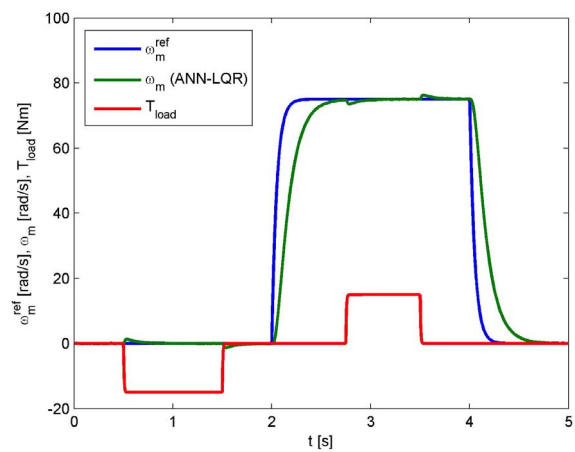

 Fig. 2. Optimal surface for  $\mathbf{K}(1,1)$  controller gain

 Fig. 4. Optimal surface for  $\mathbf{K}(2,3)$  controller gain

 Fig. 3. Optimal surface for  $\mathbf{K}(1,2)$  controller gain

 Fig. 5. Optimal surface for  $\mathbf{K}(2,4)$  controller gain

coordinates described in [18] and stator resistance adaptation scheme were employed. Flux angular velocity and slip speed are calculated from following equations:

$$a_1 = \omega_{\psi_s} = \frac{d}{dt} \arctan \left( \frac{\hat{\psi}_{s\beta}}{\hat{\psi}_{s\alpha}} \right) = \\ = \frac{(u_{s\beta} - \hat{R}_s i_{s\beta}) \hat{\psi}_{s\alpha} - (u_{s\alpha} - \hat{R}_s i_{s\alpha}) \hat{\psi}_{s\beta}}{\hat{\psi}_{s\alpha}^2 + \hat{\psi}_{s\beta}^2} \quad (5)$$

$$a_2 = \omega_{\psi_s} - p_b \omega_m \quad (6)$$

where:  $\bullet_\alpha, \bullet_\beta$  denotes components in stationary orthogonal reference frame fixed to the stator,  $\bullet$  indicates estimated values. Fig. 2-5 show examples of optimal control surfaces for selected gains. Fig. 6-8 show speed, flux and current responses of the drive under correct parameter identification. All currents shown in figures are observed in stationary reference frame fixed to the stator. Conversion between stationary ( $\alpha\beta$ ) and rotating ( $xy$ ) reference frames is given


 Fig. 6. Speed response of the drive under exact parameter identification ( $R_s = \hat{R}_s, R_r = \hat{R}_r, J = \hat{J}$ )

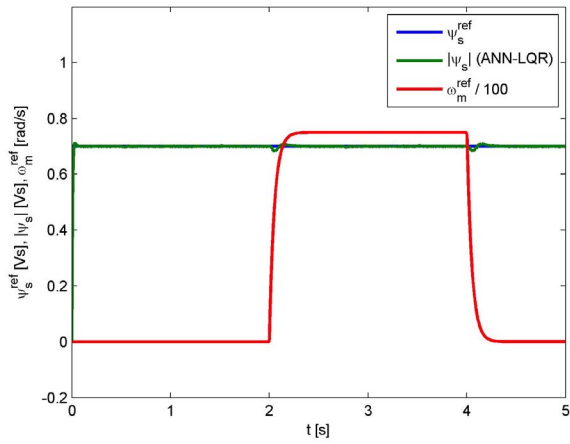


Fig. 7. Flux response of the drive under exact parameter identification ( $R_s = \hat{R}_s$ ,  $R_r = \hat{R}_r$ ,  $J = \hat{J}$ )

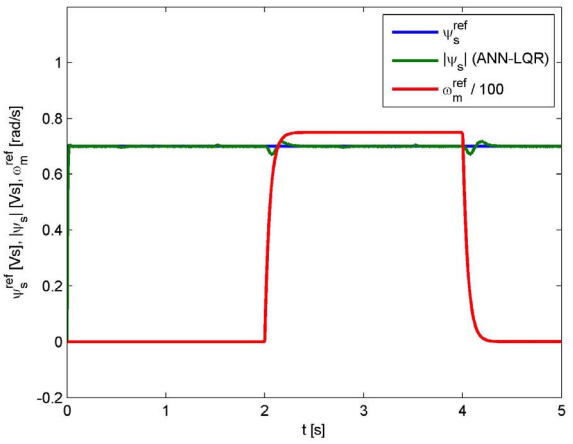


Fig. 10. Flux response of the drive under incorrect stator and rotor resistances identification ( $R_s = 2\hat{R}_s$ ,  $R_r = 2\hat{R}_r$ )

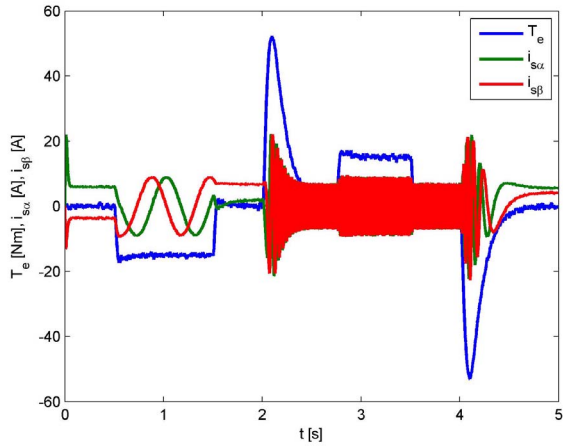


Fig. 8. Current and torque responses of the drive under exact parameter identification ( $R_s = \hat{R}_s$ ,  $R_r = \hat{R}_r$ ,  $J = \hat{J}$ )

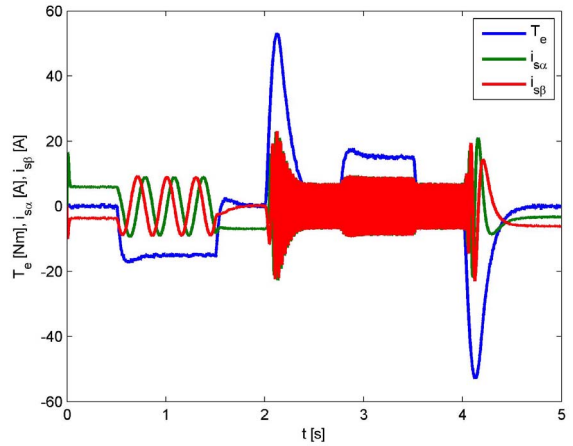


Fig. 11. Current and torque responses of the drive under incorrect stator and rotor resistances identification ( $R_s = 2\hat{R}_s$ ,  $R_r = 2\hat{R}_r$ )

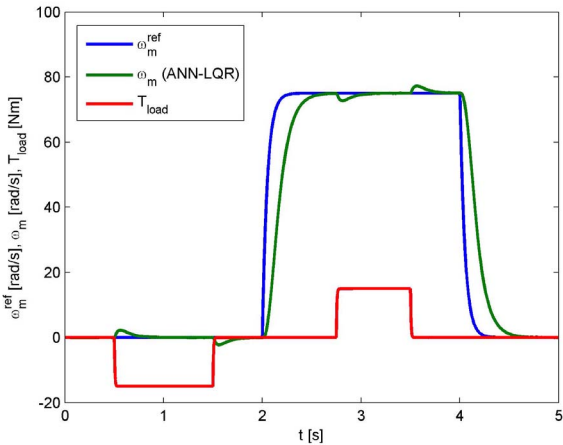


Fig. 9. Speed response of the drive under incorrect stator and rotor resistances identification ( $R_s = 2\hat{R}_s$ ,  $R_r = 2\hat{R}_r$ )

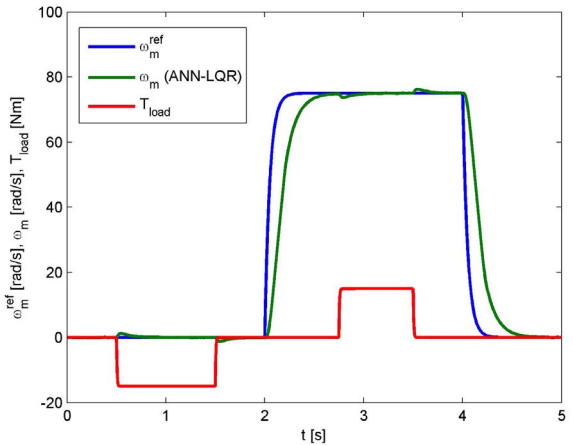


Fig. 12. Speed response of the drive under incorrect inertia identification ( $J = 1.5\hat{J}$ )

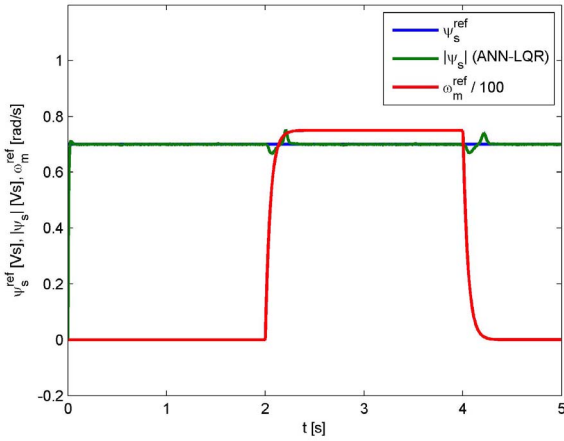


Fig. 13. Flux response of the drive under incorrect inertia identification ( $J = 1.5\hat{J}$ )

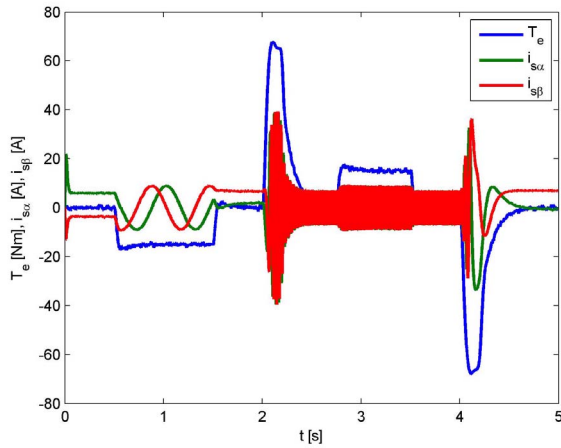


Fig. 14. Current and torque responses of the drive under incorrect inertia identification ( $J = 1.5\hat{J}$ )

by following equations:

$$\begin{aligned} i_{s\alpha} &= i_{sx} \cos \phi - i_{sy} \sin \phi \\ i_{s\beta} &= i_{sx} \sin \phi + i_{sy} \cos \phi \end{aligned}$$

where  $\phi = \int_0^t \omega_{\psi_s}(t) dt$ .

Performance of the drive under parameter mismatch was tested. Behavior of the system in case of stator and rotor resistances rise in amount of 100% is depicted in Fig. 9-11. Results of the test for moment of inertia 50% higher than the one set in **A** and **B** matrices are illustrated in Fig. 12-14. Robustness against reasonable parameters variations and almost decoupled control of flux and speed was observed.

#### IV. FURTHER RESEARCH

In future work constraint control problem have to be addressed. Any drive control system should give possibility to set hard limits for current (or torque). One can decrease

currents in described system by increasing penalty coefficients related to  $i_{sx}$  and  $i_{sy}$ . Nevertheless, hard limits cannot be achieved by playing with **Q**, **R** and **N** matrices. Experimental setup is planned to be built. Stability issues have to be discussed in detail and global stability should be ensured theoretically.

#### V. CONCLUSIONS

Novel state feedback controller for induction motor drive has been proposed and tested. Optimal, in terms of cost function minimization, control law has been achieved. Design method dedicated to LTI systems has been successfully extended to non-stationary nonlinear system, namely induction motor. Twelve gains of the controller vary with operating point of the drive. The controller was optimized for 10000 operating points defined by stator flux and rotor angular speeds. Artificial neural network stores (compresses) information on these gains and provides (thanks to knowledge generalization) controller gains for any operating point. Surfaces determined by individual gains are rather smooth, which, in turn, justifies the statement that the elaborated controller can be regarded as optimal in any reasonable operating point of the machine. Its optimality comes from soft switching between gains optimized for representative operating points. Local stability is ensured in the sense of all local models with poles in left half-plane. The ANN is of MLP (FFNN) type and consists of a dozen or so neurons. From computational time point of view, proposed control strategy is suitable for real time implementation. Robustness against significant identification errors has been observed. Experimental evaluation is currently planned.

#### APPENDIX

All included in the paper results are linked to the induction motor with parameters given in Table I.

TABLE I  
INDUCTION MOTOR PARAMETERS

Parameter	Symbol	Unit	Value
Type of rotor	-	-	squirrel-cage
Nominal power	-	kW	1.5
Nominal voltage	$U_N$	V	127/220
Nominal current	$I_N$	A	12.0/6.9
Nominal speed	$\omega_N$	rad/s	97
Number of pole pairs	$p_b$	-	3
Stator resistance	$R_s$	$\Omega$	1.54
Rotor resistance	$R_r$	$\Omega$	1.29
Stator inductance	$L_s$	mH	100.4
Rotor inductance	$L_r$	mH	96.9
Mutual inductance	$L_m$	mH	91.5
Moment of inertia	$J$	$\text{kg m}^2$	0.15

#### REFERENCES

- [1] M. Zelechowski, "Space vector modulated - direct torque controlled (DTC-SVM) inverter-fed induction motor drive," Ph.D. dissertation, Warsaw University of Technology, Faculty of Electrical Engineering, 2005.

- [2] G. Buja and M. Kazmierkowski, "Direct torque control of PWM inverter-fed AC motors - a survey," *IEEE Transactions on Industrial Electronics*, vol. 51, no. 4, pp. 744–757, August 2004.
- [3] M. Włas and A. Lewicki, "Dynamic performance of sensorless induction motor drives with two control systems based on multiscalar models," in *Proc. CD-ROM of 11th European Conference on Power Electronics and Applications (EPE)*, Dresden, September 2005.
- [4] M. Włas, Z. Krzeminski, J. Guzinski, H. Abu-Rub, and H. Toliyat, "Artificial-neural-network-based sensorless nonlinear control of induction motors," *IEEE Transactions on Energy Conversion*, vol. 20, pp. 520 – 528, September 2005.
- [5] L. Grzesiak, V. Meganck, J. Sobolewski, and B. Ufnalski, "DTC-SVM drive with ANN-based speed controller," in *Proc. of International Conference on Power Electronics and Intelligent Control for Energy Conservation (PELINCEC)*, Warsaw University of Technology, Poland, October 2005.
- [6] F. Grasser, A. D'Arrigo, S. Colombi, and A. Rufer, "JOE: a mobile, inverted pendulum," *IEEE Transactions on Industrial Electronics*, vol. 49, no. 1, pp. 107 – 114, February 2002.
- [7] B. Sprenger, L. Kucera, and S. Mourad, "Balancing of an inverted pendulum with a SCARA robot," *IEEE/ASME Transactions on Mechatronics*, vol. 3, no. 2, pp. 91 – 97, June 1998.
- [8] R. Ehrlich, J. Adler, and H. Hindi, "Rejecting oscillatory, non-synchronous mechanical disturbance in hard disk drives," *IEEE Transactions on Magnetics*, vol. 37, no. 2, pp. 646 – 650, March 2001.
- [9] F. Profumo, M. Madlena, and G. Griva, "State variables controller design for vibrations suppression in electric vehicles," in *Proc. of 27th Annual IEEE Power Electronics Specialists Conference (PESC)*, vol. 2, June 1996, pp. 1940 – 1947.
- [10] C. Jacobina, A. Lima, and F. Salvadori, "Flux and torque control of an induction machine using linear discrete state space approach," in *Proc. of 23rd International Conference on Industrial Electronics, Control and Instrumentation (IECON)*, vol. 2, November 1997, pp. 511 – 516.
- [11] C. Bottura and S. Filho, "Robust torque tracking control for the induction machine," in *Proc. of the 24th Annual Conference of the IEEE Industrial Electronics Society, IECON*, vol. 3, August/September 1998, pp. 1533 – 1537.
- [12] M. Denai and A. Draou, "Robust LQGI speed control of induction motor," in *Proc. of 5th International Workshop on Advanced Motion Control (AMC)*, Coimbra, 29 June – 1 July 1998, pp. 99 – 102.
- [13] M. Denai and S. Attia, "Robust fuzzy state feedback control of a field oriented induction motor," in *Proc. of 6th International Workshop on Advanced Motion Control (AMC)*, Nagoya, 30 March – 1 April 2000, pp. 281 – 286.
- [14] ——, "Fuzzy and neural control of an induction motor," *International Journal of Applied Mathematics and Computer Science (AMCS)*, vol. 12, no. 2, pp. 221–233, 2002.
- [15] ——, "Intelligent control of an induction motor," *Electric Power Components and Systems (Taylor & Francis)*, vol. 30, no. 4, pp. 409–427, April 2002.
- [16] *MATLAB/Simulink R14 manual*, The MathWorks, Inc., 2005. [Online]. Available: <http://www.mathworks.com/>
- [17] *PLECS Manual*, PLEXIM GmbH. [Online]. Available: [www.plexim.com](http://www.plexim.com)
- [18] J. Hu and B. Wu, "New integration algorithms for estimating motor flux over a wide speed range," *IEEE Transactions on Power Electronics*, vol. 13, no. 5, pp. 969–977, September 1998.